

## Active Vibration Control using Piezoelectric Actuator: Implementation of Ant Colony Optimization Technique in Virtual Experimentation

Khairul A. M. Nor<sup>1</sup>, Asan G. A. Muthalif<sup>2</sup>, Azni N. Wahid

*Smart Structures, Systems & Control Research Laboratory, Department of Mechatronics Engineering,*  
International Islamic University Malaysia

Jalan Gombak, 53100, Kuala Lumpur, Malaysia

<sup>1</sup>[affendy@iium.edu.my](mailto:affendy@iium.edu.my), <sup>2</sup>[asan@iium.edu.my](mailto:asan@iium.edu.my)

**Abstract**—This paper demonstrates the implementation of virtual experiment using COMSOL Multiphysics – MATLAB integration for optimization in active vibration control system. The benchmark model is a simply supported thin plate excited and attenuated by two piezoelectric patches. Instead of using equation-based modeling to represent the system, optimization of the sensor-actuator location and controller gains are conducted directly on the finite element model in COMSOL Multiphysics via *Livelink for MATLAB* function. The optimization is based on the average energy reduction across a frequency range between 11 Hz to 50 Hz, which covers the first three modes. It is found that the maximum attenuation achieved is 68.31% using optimal values of sensor-actuator location and controller gains.

**Keywords**-COMSOL Multiphysics – MATLAB integration; Livelink for MATLAB; active vibration control; Ant Colony Optimization

### I. INTRODUCTION

Active vibration control (AVC) is a technique to suppress vibration by giving the actuating force in the opposite direction of the disturbance force with the help of feedback control. This AVC technique combined with the smart actuators such as piezoelectric material, shape memory alloy (SMA) and magneto-rheological fluid (MRF) enable researchers to produce light-weight yet stronger and more flexible structures. The performance of AVC system can be further enhanced by using the optimized parameters of the system or controller. Apart from the successes reported in optimization using common optimization techniques such as linear quadratic regulator (LQR) [1], H2 norms [2-3] and H (infinity) norm [4], the use of biologically-inspired optimization algorithm in AVC system has gained significant attention due to its reliability. One of them is Ant Colony Optimization (ACO) [5-7]. ACO algorithm is inspired by the behavior of real ants in which the ants uses pheromones as a communication medium in finding food source [8].

In term of modeling a system, equation-based modeling is normally preferred for established substructures such as rectangular, circle, etc. In contrast, complex structures are easily modeled using finite element software but the computational cost is relatively high. One of the powerful features in COMSOL Multiphysics software; a commercially available finite element package, is the ability to modify the parameters of its finite element model from within the MATLAB's scripting environment via *Livelink for MATLAB* function. This integration is realizable either by using MATLAB as scripting interface to set up and solve the COMSOL Multiphysics models, or by calling MATLAB functions when modeling within the COMSOL Multiphysics desktop. As a result, it is deemed possible to employ MATLAB-coded controller algorithm to virtually control vibration in a finite element model developed in COMSOL

Multiphysics. This also enables us to optimize the physical parameters of the finite element model as well as the controller parameters.

This paper presents optimization of sensor-actuator location and PID controller gains in AVC system. The benchmark model is a simply-supported rectangular plate attached with two piezoelectric patches (as vibration exciter and suppressor) developed in finite element software namely COMSOL Multiphysics. Optimization is conducted by interfacing the ACO algorithm written in MATLAB to the said benchmark model. This paper is arranged as follows. Section II presents the equation of motion (EOM) of the system. Verification of finite element results and integration between COMSOL Multiphysics and MATLAB software is discussed in detail in Section III. Section IV focuses on optimization and comprises of explanation on the ACO algorithm and objective function, as well as discussions on optimizing the location of the collocated sensor-actuator and the controller gains. The selected optimal values are based on the highest reduction of frequency-averaged energy.

### II. MATHEMATICAL MODELING

The constitutive equation of piezoelectric material as actuator is [9]:

$$\sigma = c^E \epsilon - eE \quad (1)$$

where  $\sigma$  is the stress vector,  $c^E$  is the matrix of elastic coefficients under constant electric field,  $\epsilon$  is the strain vector,  $e$  is the dielectric permittivity matrix and  $E$  is the electric field vector. Considering the piezoelectric patch as a linear isotropic material, therefore (1) can be expanded to:

$$\begin{bmatrix} \sigma_{xx} \\ \sigma_{yy} \\ \sigma_{xy} \end{bmatrix} = \begin{bmatrix} \frac{E_p \nu_{pz}}{1-\nu_{pz}^2} & \frac{\nu_{pz} E_p}{1-\nu_{pz}^2} & 0 \\ \frac{\nu_{pz} E_p}{1-\nu_{pz}^2} & \frac{E_p}{1-\nu_{pz}^2} & 0 \\ 0 & 0 & \frac{E_p}{2(1+\nu_{pz})} \end{bmatrix} \begin{bmatrix} \epsilon_{xx} \\ \epsilon_{yy} \\ \epsilon_{xy} \end{bmatrix}$$

$$- \begin{bmatrix} \frac{E_p \nu_{pz}}{1-\nu_{pz}^2} & \frac{\nu_{pz} E_p}{1-\nu_{pz}^2} & 0 \\ \frac{\nu_{pz} E_p}{1-\nu_{pz}^2} & \frac{E_p}{1-\nu_{pz}^2} & 0 \\ 0 & 0 & \frac{E_p}{2(1+\nu_{pz})} \end{bmatrix} \begin{bmatrix} d_{31} \\ d_{32} \\ 0 \end{bmatrix} \frac{V(t)}{t_p} \quad (2)$$

where  $d_{31}$  and  $d_{32}$  are the piezoelectric strain constants ( $d_{31} = d_{32}$ , because of isotropic),  $E_p$  and  $\nu_{pz}$  are the Young's modulus for plate and piezoelectric patch, respectively, and  $\nu_{pz}$  are the Poisson's ratio for plate and piezoelectric patch, respectively,  $V(t)$  is voltage supplied to the piezoelectric actuator and  $t_p$  is the piezoelectric patch thickness.

In the case of a simply supported plate at all edges, the deflection of the plate during vibration is represented as the summation of modes in double series [10]:

$$w(x, y) = \sum_m \sum_n W_{mn} \sin \frac{m\pi x}{a} \sin \frac{n\pi y}{b} \quad (3)$$

where  $W_{mn}$  is the magnitude and subscripts  $m$  and  $n$  refer to half-wave number in the  $x$  and  $y$  directions, respectively. Lagrange's method is employed to derive the equation of motion of a simply supported plate with attached piezoelectric patch. Thus, the equation of motion of plate with 2 patches is written as:

$$(-\omega^2 \mathbf{M} + \mathbf{K}_c) \mathbf{w}_{mn} = \mathbf{f}_e + \mathbf{f}_c \quad (4)$$

where  $\omega$  is angular frequency in rad/s,  $\mathbf{M}$  is mass matrix,  $\mathbf{K}_c$  is stiffness matrix,  $\gamma$  is modal loss factor,  $i$  is imaginary unit,  $\mathbf{w}_{mn}$  is the modal amplitude vector, and  $\mathbf{f}_e$  and  $\mathbf{f}_c$  are the modal force vector generated by exciter and controller patches, respectively.

### III. ACTIVE VIBRATION CONTROL USING COMSOL MULTIPHYSICS – MATLAB INTEGRATION

#### A. Building the benchmark model using COMSOL Multiphysics

A simply-supported rectangular thin plate attached with two piezoelectric patches is modeled in COMSOL Multiphysics and equipped with *piezoelectric devices* physics interface. Details of the said model are given in Table I. The model structure is meshed using *triangular mesh* with 3428 number of elements.

TABLE I. COMSOL MULTIPHYSICS MODEL PARAMETERS

Parameters	Plate (Stainless Steel)	Piezoelectric patch (PZT-5A)
Length	0.5 m	0.05 m
Width	0.6 m	0.02 m
Thickness	0.001 m	0.0001 m
Density	7850 kg/m <sup>3</sup>	7750 kg/m <sup>3</sup>
Young's Modulus	200e9 N/m <sup>2</sup>	70e9 N/m <sup>2</sup>
Poisson's ratio	0.33	0.31
piezoelectric constants, $d_{31}$	-	-171e-10 C/N
piezoelectric constants, $d_{32}$	-	-171e-10 C/N
Loss factor	0.05	0.05

The plate energy (denoted by EP) is calculated by integrating the energy density for the whole system, i.e. plate and piezoelectric patches; over the volume using the following equation.

$$EP = \iiint \frac{1}{2} \rho (u^2 + v^2 + w^2) dV \quad (5)$$

where  $\rho$  is the density,  $V$  is the volume,  $u$ ,  $v$ , and  $w$  are the velocity in  $x$ ,  $y$  and  $z$  directions, respectively. Thus, the frequency-averaged energy for a certain frequency range can be calculated using

$$(6)$$

where  $\bar{E}_p$  is the frequency-averaged plate energy, and  $\omega_i$  and  $\omega_f$  are the initial and final frequencies, respectively.

#### B. Verification of finite element results

The results in free and force vibration obtained from finite element method via COMSOL Multiphysics software are verified with analytical method developed in Section II earlier. For this purpose, frequency range of 0 to 200 Hz is used.

##### 1) Free Vibration

Sixteen natural frequencies for free flexural vibration of the plate using analytical method via MATLAB and finite element method via *Eigenfrequency study* function in COMSOL Multiphysics, are compared and tabulated in Table II. The results show that, both methods produce similar natural frequencies, especially in lower frequencies, but the differences are increasing for higher frequencies.

##### 2) Force Vibration

Comparison for force vibration is done by considering excitation of the plate with two types of excitation. One is by point force located at (0.15 m, 0.15 m) with magnitude of force of 1 N. The other one is by piezoelectric patch located at (0.15 m, 0.15 m) measured from patch centre, with voltage supply of 100 V. Displacement response measured at the plate centre and the energy response between both analytical and FE models excited by point force and piezoelectric patch are plotted in Figs. 1 and 2, respectively. Based on the figures, the responses between analytical and finite element method are almost similar.

TABLE II. COMPARISON OF NATURAL FREQUENCIES USING ANALYTICAL AND FINITE ELEMENT METHODS

Mode	Frequency (Hz)		% difference
	Analytical (MATLAB)	Finite Element (COMSOL Multiphysics)	
1	16.269	16.561	1.764
2	36.324	36.924	1.626
3	45.164	46.162	2.162
4	65.233	66.697	2.195
5	69.500	71.662	3.018
6	92.850	96.319	3.601
7	98.244	102.009	3.690
8	112.815	116.806	3.416
9	116.193	119.894	3.087
10	144.995	150.394	3.590
11	146.330	153.201	4.485
12	160.154	168.561	4.988
13	176.487	185.647	4.934
14	180.254	189.386	4.822
15	192.918	203.459	5.181
16	205.451	216.455	5.084

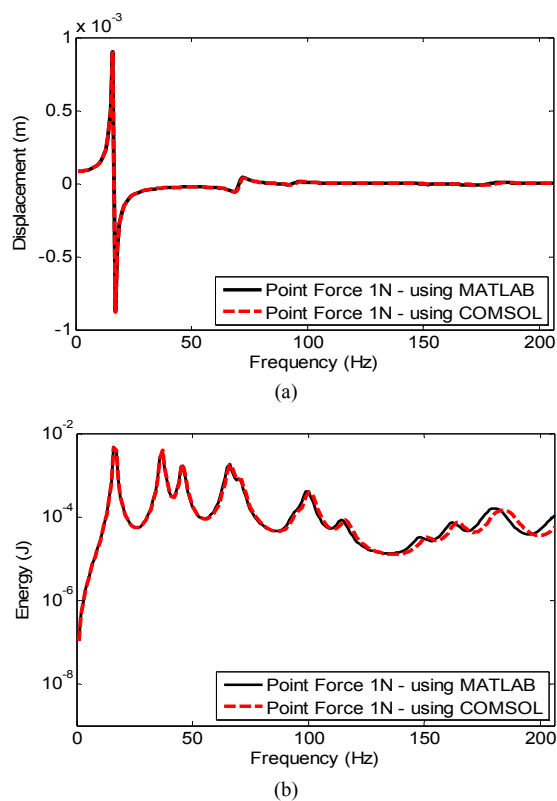


Figure 1. Comparison of numerical results for vibration excited using point force: (a) Displacement at plate centre and (b) Energy

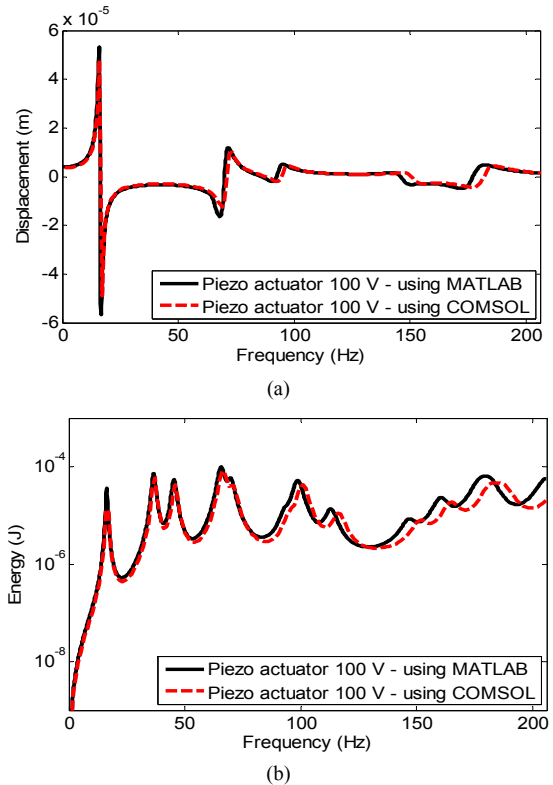


Figure 2. Comparison of numerical results for vibration excited using piezoelectric patch: (a) Displacement at plate centre and (b) Energy

C. Interfacing of MATLAB-coded controller with COMSOL Multiphysics model

This section discusses the interfacing of MATLAB-coded controller with COMSOL Multiphysics model. The benchmark model developed in COMSOL Multiphysics is loaded into MATLAB scripting environment using *Livelink for MATLAB* function. The exciter patch is powered by 100 V and located at (0.15 m, 0.15 m) while the controller patch's location is determined using optimization technique described in Section IV. To actively control vibration of the benchmark model, a PID controller with collocated sensor-actuator configuration is developed in MATLAB script and used to manipulate the voltage of the controller patch in the model. Velocity at the sensor-actuator location for uncontrolled system is taken as the input of the controller, which is used to generate the voltage of the controller patch (denoted by  $v_c$ ) as follows:

$$v_c = k_p * (0 - v_{ms}) + k_i * \int (0 - v_{ms}) dt + k_d * \frac{d(0 - v_{ms})}{dt} \quad (7)$$

where  $k_p$ ,  $k_i$  and  $k_d$  are the PID controller gains, and  $v_{ms}$  is the velocity of uncontrolled system measured from sensor-actuator location. This interfacing is illustrated in Fig. 3.

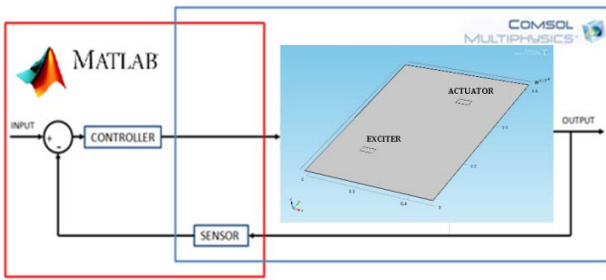


Figure 3. Integration of COMSOL Multiphysics and MATLAB.

IV. OPTIMIZATION

A. Ant Colony Optimization algorithm

Simple-ACO (SACO), a variation of ACO, is employed in this paper. Global cooperation among ants in a colony can produce promising paths towards the food source by using pheromones as a communication medium. An ant deposits pheromone trails on the ground while looking for the food. The next ants will tend to follow the stronger trails and also reinforcing the trail with their own pheromone, which consequently making the path more favorable as compared to others. Meanwhile, the weaker trails progressively decreased by evaporation.

The probability equation in SACO can be written as:

$$P_k(t) = \begin{cases} \frac{[\tau_{ij}(t)]^\alpha}{\sum_{l \in T_k} [\tau_{ij}(t)]^\alpha} & , \text{if } j \in T_k \\ 0 & , \text{otherwise} \end{cases} \quad (8)$$

where  $\tau_{ij}$  is the pheromone trail,  $t$  is time,  $\alpha$  is the constant that defines the relative importance of the pheromone values and  $T_k$  is the path effectuated by the ant  $k$  at a given time. The value of tour taken by each ant is:

$$\Delta\tau_{ij}(t) = \begin{cases} \frac{Q}{L_k} & , \text{if } (i,j) \text{ walked by ant } k \\ 0 & , \text{otherwise} \end{cases} \quad (9)$$

where  $Q$  is a constant and  $L_k$  is the cost of tour by ant  $k$  or the objective function. In this paper,  $L_k$  is the inverse of energy reduction. The pheromone trails are updated using:

$$\tau_{ij}(t) = \rho\tau_{ij}(t-1) + \sum_{k=1}^{NA} \Delta\tau_{ij}(t) \quad (10)$$

where  $\rho$  is the pheromone decay to introduce the forgetfulness of the bad choices and  $NA$  is the number of ants. The ACO parameters used throughout the paper are listed in Table III. The flowchart of the SACO algorithm is shown in Fig. 4.

TABLE III. ACO PARAMETERS

Parameter	Value
Number of ants	5
Maximum generation	10
$\alpha$	1
Pheromone decay,	0.95

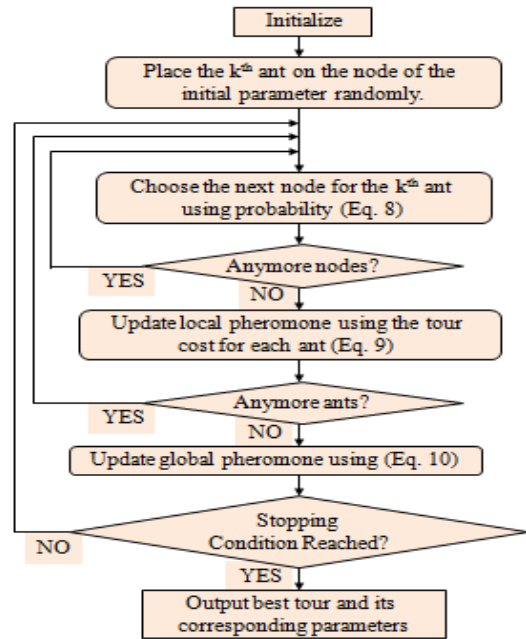


Figure 4. Flowchart of SACO.

B. Objective Function

The objective function in this paper is to maximize the energy reduction (denoted by ER), which can be defined as

$$\text{maximize } ER = \frac{HE_{nc} - HE_c}{HE_{nc}} \quad (11)$$

where  $HE_{nc}$  and  $HE_c$  are the average plate energy with and without control, respectively. The frequency range of interest for optimization is between 11 Hz to 50 Hz, which covers the first three modes.

All optimization are computed on a 2.20 GHz Intel® Core™ i7 processor with 8 GB of random access memory. Since optimization of five variables ( $x$ ,  $y$ ,  $k_p$ ,  $k_i$  and  $k_d$ ) is computationally expensive, the process is conducted in two stages as follows:

1) Two variables,  $x$ - and  $y$ -coordinates of the collocated sensor-actuator ( $x_{sa}, y_{sa}$ ), are optimized while applying simple velocity feedback control with an initial gain of 4850, which is approximately equal to 50 times of the infinite plate driving point impedance.

2) The remaining three variables,  $k_p$ ,  $k_i$  and  $k_d$  of the PID controller are determined while fixing location of sensor-actuator with the values found in the first step.

C. Optimal sensor-actuator location

There is a very high chance that the optimization algorithm will end up choosing location near the exciter patch i.e. location of the disturbance; as the optimal sensor-actuator location. This is because the best way to reduce vibration is by directly locking the disturbance force [11]. However, this is not practical because in reality it is difficult to know the origin of disturbance. Having said that, it is made a condition that the controller patch must be placed 0.05 m apart along x and y axes from the exciter patch. The variables to be optimized i.e.  $(x_{sa}, y_{sa})$ , are coded by 10000 nodes making 10000 x 10000 possible combinations.

The energy plots obtained using different sensor-actuator location and the corresponding energy reduction with respect to the mode are shown in Fig. 5(a) and Fig. 5(b), respectively. Based on these figures, locations of sensor-actuator are varied if one wants to reduce vibration at a particular mode. Table IV shows energy reduction with respect to different sensor-actuator locations. For mode number 1, 2 and 3, the best sensor-actuator locations are at (0.2097 m, 0.2760 m), (0.3504 m, 0.4370 m) and (0.3504 m, 0.3901 m), respectively. However, considering broadband vibration attenuation within the frequency range of interest (11 Hz to 50 Hz), the optimal location to place the controller patch is at (0.3519 m, 0.4132 m) with frequency-averaged energy reduction of 41.51%. Fig. 6 shows the convergence plot for sensor-actuator location optimization.

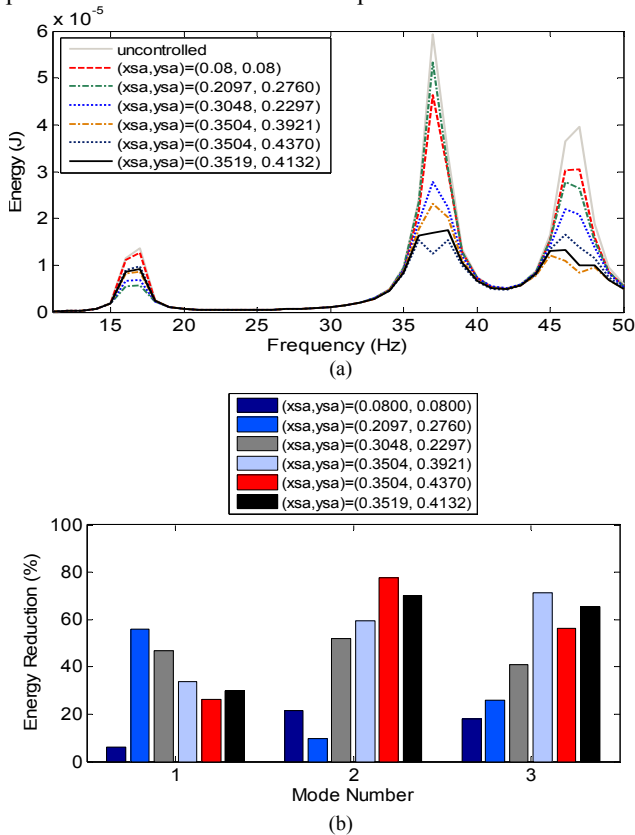


Figure 5. (a) Energy plot and (b) energy reduction with respect to mode, using different sensor-actuator locations.

TABLE IV. ENERGY REDUCTION WITH RESPECT TO DIFFERENT SENSOR-ACTUATOR LOCATIONS

Sensor-actuator location		Energy reduction (%)			
$x_{sa}$ (m)	$y_{sa}$ (m)	1st mode	2nd mode	3rd mode	Frequency-averaged
0.0800	0.0800	5.94	21.40	18.05	10.51
0.2097	0.2760	56.12	9.83	25.71	13.49
0.3048	0.2297	46.78	51.98	40.94	28.40
0.3504	0.3921	33.62	59.67	71.50	40.12
0.3504	0.4370	26.19	77.58	56.28	40.92
<b>0.3519</b>	<b>0.4132</b>	<b>29.90</b>	<b>70.04</b>	<b>65.43</b>	<b>41.51</b>

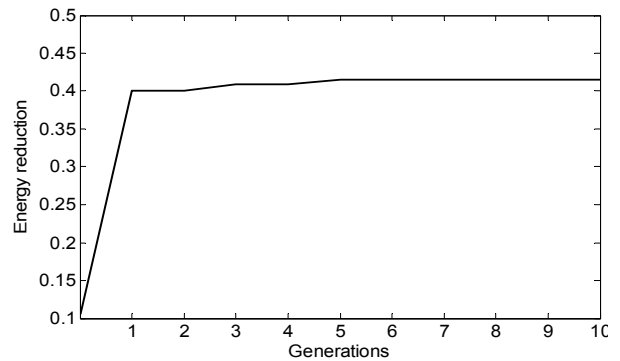


Figure 6. Convergence plot for optimization of sensor-actuator location.

D. Optimal PID controller gains

Optimization of PID gains is conducted while considering the optimal sensor-actuator, which is (0.3519 m, 0.4132 m). The range of values for  $k_p$ ,  $k_i$  and  $k_d$  obtained are 1000 to 20000, 1000 to 2000 and 0.1 to 10, respectively. Each parameter is coded by 10000 nodes making 10000 x 10000 possible combinations.

Figs. 7(a) and 7(b) illustrate the energy plots obtained using different PID gains while fixing the controller patch at its optimal location and the bar graph of the corresponding amount of energy attenuation in percentage for each mode, respectively. Overall, the result presented in Table V shows improvement in energy reduction as compared to attenuation using velocity feedback controller in the previous section. This is proven by the increasing of the maximum frequency-averaged energy reduction to 68.31 % by tuning the  $k_p$ ,  $k_i$  and  $k_d$  values to 12211, 11511 and 4.6158, respectively. For this controller optimization, the convergence profile of the objective function is depicted in Fig. 8.

TABLE V. ENERGY REDUCTION WITH RESPECT TO DIFFERENT PID GAINS

PID gains			Energy reduction (%)			
$k_p$	$k_i$	$k_d$	1st mode	2nd mode	3rd mode	Frequency-averaged
4850	1000.0	0.1000	29.91	70.00	65.40	41.56
9948	4243.6	4.3594	54.65	97.07	95.52	65.35
13448	17819	3.4198	67.81	88.97	88.74	68.07
12211	10309	4.7634	63.58	94.64	93.80	68.30
<b>12211</b>	<b>11511</b>	<b>4.6158</b>	<b>63.55</b>	<b>94.62</b>	<b>93.81</b>	<b>68.31</b>

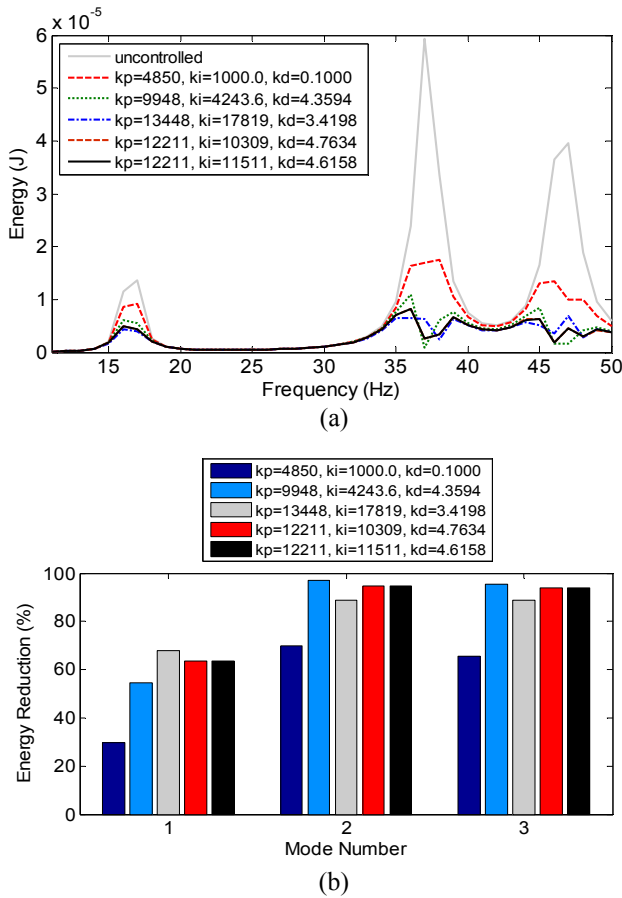


Figure 7. (a) Energy plot and (b) energy reduction with respect to mode, using different PID gains.

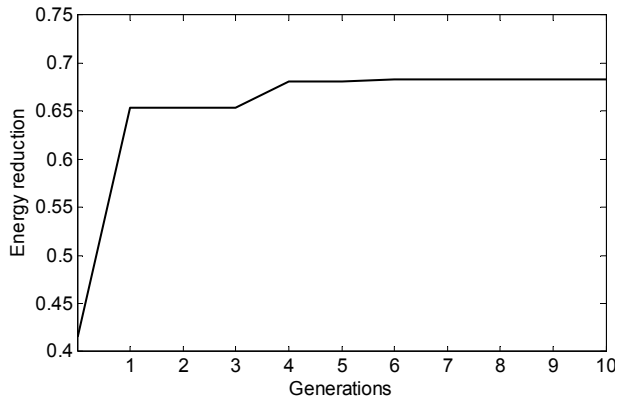


Figure 8. Convergence plot for optimization of PID controller gains.

V. CONCLUSION

Verification of the mathematical model with COMSOL Multiphysics model has been made whereby both models produced similar responses, especially in lower frequencies. Optimization of collocated sensor-actuator location and PID controller gains using COMSOL Multiphysics – MATLAB integration is successfully performed with time taken to complete each optimization is about 8.25 hours. It is

expected that, better results can be obtained if more ‘ants’ and number of iterations in ACO algorithm are used, however the computational cost will inevitably be high.

REFERENCES

- [1] P. Bhattacharya, *et al.*, "Finite element analysis and distributed control of laminated composite shells using LQR/IMSC approach," *Aerospace Science and Technology*, vol. 6, pp. 273-281, 2002.
- [2] M. A. Demetriou, "A numerical algorithm for the optimal placement of actuators and sensors for flexible structures," in *American Control Conference, 2000. Proceedings of the 2000*, 2000, pp. 2290-2294 vol.4.
- [3] W. Gawronski, "Actuator and sensor placement for structural testing and control," *Journal of Sound and Vibration*, vol. 208, pp. 101-109, 1997.
- [4] T. L. da Rocha, *et al.*, "Optimal Location of Piezoelectric Sensor and Actuator for Flexible Structures," in *11th International Congress on Sound and Vibration, Russia, 2004*, pp. 1807-1814.
- [5] M. Mohamad, *et al.*, "Continuous ant colony optimisation for active vibration control of flexible beam structures," in *Mechatronics (ICM), 2011 IEEE International Conference on*, 2011, pp. 803-808.
- [6] S. Julai and M. Tokhi, "Active vibration control of flexible plate structures with distributed disturbances," *Journal of Low Frequency Noise, Vibration and Active Control*, vol. 31, pp. 123-150, 2012.
- [7] H. Nobahari, *et al.*, "Hardware-in-the-loop optimization of an active vibration controller in a flexible beam structure using evolutionary algorithms," *Journal of Intelligent Material Systems and Structures*, p. 1045389X13502874, 2013.
- [8] M. Dorigo and T. Stützle, *Ant Colony Optimization*. MIT Press, Bradford Books, 2004.
- [9] A. Preumont, *Vibration Control of Active Structures : An Introduction*, Third ed.: Springer, 2011.
- [10] S. Timoshenko and S. Woinowsky-Krieger, *Theory of plates and shells*: McGraw-Hill, 1959.
- [11] A. G. A. Muthalif and R. S. Langley, "Active control of high-frequency vibration: Optimisation using the hybrid modelling method," *Journal of Sound and Vibration*, vol. 331, pp. 2969-2983, 2012.